

## Third Law of Thermodynamics and the Scaling of Quantum Computers

Lorenzo Buffoni<sup>1</sup>,<sup>1</sup> Stefano Gherardini<sup>2,3,1</sup>, Emmanuel Zambrini Cruzeiro,<sup>4</sup> and Yasser Omar<sup>5,6,1</sup>

<sup>1</sup>*PQI—Portuguese Quantum Institute, 1049-001 Lisboa, Portugal*

<sup>2</sup>*CNR-INO, Area Science Park, Basovizza, I-34149 Trieste, Italy*


<sup>3</sup>*LENS, University of Florence, via G. Sansone 1, I-50019 Sesto Fiorentino, Italy*

<sup>4</sup>*Instituto de Telecomunicações, 1049-001 Lisboa, Portugal*

<sup>5</sup>*Instituto Superior Técnico, Universidade de Lisboa, 1049-001 Lisboa, Portugal*

<sup>6</sup>*Centro de Física e Engenharia de Materiais Avançados (CeFEMA),*

*Physics of Information and Quantum Technologies Group, 1049-001 Lisboa, Portugal*

 (Received 11 April 2022; revised 31 August 2022; accepted 1 September 2022; published 3 October 2022)

The third law of thermodynamics, also known as the Nernst unattainability principle, puts a fundamental bound on how close a system, whether classical or quantum, can be cooled to a temperature near to absolute zero. On the other hand, a fundamental assumption of quantum computing is to start each computation from a register of qubits initialized in a pure state, i.e., at zero temperature. These conflicting aspects, at the interface between quantum computing and thermodynamics, are often overlooked or, at best, addressed only at a single-qubit level. In this Letter, we argue how the existence of a small but finite effective temperature, which makes the initial state a mixed state, poses a real challenge to the fidelity constraints required for the scaling of quantum computers. Our theoretical results, carried out for a generic quantum circuit with  $N$ -qubit input states, are validated by test runs performed on a real quantum processor.

DOI: [10.1103/PhysRevLett.129.150602](https://doi.org/10.1103/PhysRevLett.129.150602)

Large-scale quantum computers represent the ultimate frontier in information processing, with the objective of obtaining quantum advantage in solving computational problems that classical computers cannot address in any feasible amount of time [1,2]. So far, one of the biggest obstacles to this endeavor has been noise, which is responsible for the decay of quantum coherence and correlations [3,4] in quantum states, especially pure states that are notoriously hard to preserve. Quantum error correction protocols [5,6], assisted by the statements of the quantum threshold theorem [7,8], can help in overcoming quantum state degradation. However, experiments on existing devices [9–11] still lack the high fidelity required for error correction. For this reason, the analysis of thermodynamic and energetic resources has recently emerged in the literature as a useful tool to study the fundamental limits of quantum computation, with several implications for quantum gates [12,13], quantum annealers [14,15], and quantum error correction [16].

In the following, we focus on thermodynamic limits for quantum state preparation, and on their consequences in obtaining high fidelity in multiqubit quantum registers. The very existence of pure states and the limits to their preparation have to face Nernst's unattainability principle, also known as the third law of thermodynamics [17], stating that cooling a physical system to the ground state ideally requires infinite resources. Since pure states can be brought to the ground state (and vice versa) by means of finite-cost transformations, i.e., unitary operations, the preparation of

pure states necessarily involves an infinite resource cost to conform to the third law. This issue has been recently brought to light in the quantum thermodynamics community with implications for quantum measurement [18], purification [19], and cooling [20]. The simplest and most fundamental case of state preparation is the initialization of a qubits register to the computational state  $|00\dots0\rangle$  by means of the operation denoted as “reset.” Single-qubit reset has been investigated in numerous platforms, some of which are solid state, such as silicon [21] or rare-earth ion-doped crystals in spin ensembles [22,23] and single ions [24], nitrogen-vacancy centers in diamond [25], superconducting qubits [26–29], microwave photons [30,31], and trapped ions [32–34]. However,  $|00\dots0\rangle$  being a pure state, it is subject to the thermodynamic constraint originated by Nernst's principle.

In this Letter, we show that in real-world quantum computers there exists a thermodynamic limit to the initialization of multiqubit registers, and consequently to the preparation of pure quantum states, that has practical implications for the scaling of quantum computers. In fact, although the reset (or initialization) of single qubits has been realized with high fidelity (even above 99.9%) [35], we will analytically prove and verify on a real device that even a small initialization error on a multiqubit register may dramatically reduce the preparation fidelity of a multiqubit state. We argue that, to scale beyond the actual devices, substantial efforts are needed to improve the quality of initialization of multiqubit registers.

*Fidelity scaling.*—The usual assumption in quantum computation is to initialize the qubits register in the computational state  $|00\dots 0\rangle$  and then evolve it with an arbitrary unitary operation. Here, we want to investigate how this operation is affected by an imperfect preparation of the initial  $|00\dots 0\rangle$  register. Using the formalism of density matrices, the initial  $N$ -qubit pure state (target state) one wishes to initialize in a quantum computer is

$$\sigma_0 \equiv \begin{pmatrix} 0 & 0 \\ 0 & 1 \end{pmatrix}^{\otimes N}, \quad (1)$$

which, by definition, is a zero temperature state. However, from Nernst's unattainability principle we are bound to prepare states that have an arbitrary small but finite temperature. Thus, we assume that the *real* initial state of the system is the thermal state  $\rho_0 = (e^{-\beta H}/Z)^{\otimes N}$  ( $Z$  is the appropriate partition function) that reads explicitly as follows:

$$\rho_0 \equiv \left[ \frac{1}{1 + e^{-\beta\Delta E}} \begin{pmatrix} e^{-\beta\Delta E} & 0 \\ 0 & 1 \end{pmatrix} \right]^{\otimes N}, \quad (2)$$

where  $\beta$  is the effective inverse temperature of the initial (prepared) state and  $\Delta E$  is the energy difference between the single-qubit states  $|0\rangle$  and  $|1\rangle$ .

It is worth noting that the effective inverse temperature  $\beta$  is not the *actual* inverse temperature of the environment in which our quantum computer is located (albeit it will depend on it), but a parameter that takes into account on average all the sources of disturbance that prevent our system from being in a perfectly pure state. For this reason, we will refer to it as an “effective” temperature. Our choice to take a global constant value for the effective inverse temperature  $\beta$ , instead of setting different inverse temperatures  $\{\beta_1, \dots, \beta_N\}$  for each qubit, stems from considering the average error on the initialization of the target state  $\sigma_0$  on all the  $N$  considered qubits for sake of clarity. Thus, without loss of generality, we can consider an average effective temperature that, in turn, makes our model easier to interpret. Moreover, let us note that with this notation, in the limit of zero temperature ( $\beta \rightarrow \infty$ ), the state  $\sigma_0$  is recovered, while in the opposite limit of infinite temperature ( $\beta \rightarrow 0$ ) one gets the maximally mixed state  $\mathbb{I}_{2^N}/2^N$ , where  $\mathbb{I}_d$  is the identity matrix of dimension  $d$ . We also recall that, given two density matrices  $\rho$  and  $\sigma$ , representing the states of a quantum system, the fidelity between them is defined as  $\mathcal{F}(\rho, \sigma) = (\text{Tr}[\sqrt{\sqrt{\rho}\sigma\sqrt{\rho}}])^2$  [36].

After setting our notation and initial assumptions, we formally show how the fundamental limit imposed by Nernst's principle on the quantum state initialization affects the scaling of quantum computers. Let us take a perfect (in the sense of noiseless) unitary transformation  $U$  operating on an ensemble of  $N$  qubits, such that  $\rho_1 \equiv U\rho_0U^\dagger$  and

$\sigma_1 \equiv U\sigma_0U^\dagger$  are the resulting density operators after the application of the transformation. Then, we can find the analytical expression for the fidelity  $\mathcal{F}(\rho_1, \sigma_1)$  as a function of the parameters  $N$  and  $\beta$ . Since the fidelity is invariant under *any* unitary transformations [37,38] and  $\sigma_0$  is a pointer state, we can prove that

$$\mathcal{F}(\rho_1, \sigma_1) = \mathcal{F}(\rho_0, \sigma_0) = \text{Tr}[\rho_0\sigma_0]. \quad (3)$$

By substituting the explicit form of  $\rho_0$  and  $\sigma_0$  in Eq. (3), the scaling of  $\mathcal{F}(\rho_1, \sigma_1)$  as a function of the parameters  $N$  and  $\beta$  is

$$\mathcal{F}(\rho_1, \sigma_1) = (1 + e^{-\beta\Delta E})^{-N}, \quad (4)$$

which is valid independently on which unitary transformation  $U$  is applied. Equation (4) shows that, even having at our disposal any perfect unitary transformation  $U$ , a value slightly bigger than zero for the initial inverse temperature  $\beta$  of the real state  $\rho_0$  can end up hindering the scaling (i.e.,  $N \rightarrow \infty$ ) of the considered quantum circuit or algorithm. The reason behind this result being so general lies again in the thermodynamic considerations behind Nernst's unattainability principle, and thus in the divergent cost of attaining a perfect pure state (i.e., with  $\beta \rightarrow \infty$ ). In fact, it now becomes clear that the issue of scaling quantum computers regards two competing limits:

$$\lim_{N \rightarrow \infty} \lim_{\beta \rightarrow \infty} \mathcal{F}(\rho_0, \sigma_0) = 1, \quad (5)$$

$$\lim_{\beta \rightarrow \infty} \lim_{N \rightarrow \infty} \mathcal{F}(\rho_0, \sigma_0) = 0. \quad (6)$$

The noncommutativity of limits is ubiquitous in statistical physics and thermodynamics [39–42], where limits taken to infinity are often relevant and often related to mechanism of spontaneous symmetry breaking. In our case, Eq. (5) states simply that if one is able to initialize a qubit in a pure quantum state, then in principle a “perfect” arbitrarily large quantum register can be realized. Instead, Eq. (6) reflects the evidence that, for finite temperature, increasing the size of the quantum device necessarily entails a decrease in the attainable initial state fidelity  $\mathcal{F}(\rho_0, \sigma_0)$  that will eventually disrupt the computation. The noncommuting nature of the two limits, Eqs. (5) and (6), is the second result of this Letter. In addition, the results of Eqs. (3) and (4) remain valid even if the real initial state  $\rho_0$  contains residual quantum coherence (in the form of off-diagonal terms) originated by nonideal state initialization routines. Refer to the Supplemental Material [43] (SM) for the proof of this further result. Accordingly, we need to prepare pure states with increasing fidelity by properly taking into account also the needed resources, at least at the energetic level. In doing this, the initialization of quantum registers would need to be

improved at a faster rate than the one at which the size of quantum computers increases.

Let us now analyze the more general case of preparing a generic pure quantum state  $|\psi\rangle$  from initializing the system in the real state  $\rho_0$ . Here, two kind of errors have to be considered: one on the initialization of  $\sigma_0$  that is quantified by the fidelity  $\mathcal{F}_I \equiv \mathcal{F}(\rho_0, \sigma_0)$ , and the other on the subsequent preparation of  $|\psi\rangle$ . For the latter, the source of error stems from the fact the unitary operator  $U$ , needed for the preparation of  $|\psi\rangle$ , will be subjected to environmental noise in the form of a nonunitary quantum map  $\Phi$ . This second error is quantified by the fidelity

$$\mathcal{F}_P \equiv \mathcal{F}(s_1, |\psi\rangle\langle\psi|) = \langle 0|U^\dagger\Phi(\sigma_0)U|0\rangle, \quad (7)$$

where  $s_1 \equiv \Phi(\sigma_0)$  and  $|0\rangle \equiv |00\dots 0\rangle$  for convenience. Hence, our aim is to have some information on the scaling of the fidelity  $\mathcal{F}(\rho_1, |\psi\rangle\langle\psi|) = \langle 0|U^\dagger\Phi(\rho_0)U|0\rangle$  as a function of  $N$ , with  $\rho_1 \equiv \Phi(\rho_0)$ . The quantity  $\mathcal{F}(\rho_1, |\psi\rangle\langle\psi|)$  is thus the fidelity of the composite process “initialization + preparation.” As demonstrated in the SM [43]  $\mathcal{F}(\rho_1, |\psi\rangle\langle\psi|)$  is bounded from below and above by functions depending only on  $\mathcal{F}_I$  and  $\mathcal{F}_P$ :

$$\mathcal{F}_P\mathcal{F}_I \leq \mathcal{F}(\rho_1, |\psi\rangle\langle\psi|) \leq \min\{\mathcal{F}_P, \mathcal{F}_I\}. \quad (8)$$

As a result, irrespective of the gate fidelity  $\mathcal{F}_P$ , whose computation requires some knowledge of  $\Phi$ , both the lower and upper bounds of  $\mathcal{F}(\rho_1, |\psi\rangle\langle\psi|)$  scale at least with  $\mathcal{F}_I = (1 + e^{-\beta\Delta E})^{-N}$ , namely exponentially in  $N$ . This is the third main result of this Letter, which should further clarify the impact of Nernst’s unattainability principle for the preparation of a pure quantum state in a real setting.

To reinforce the result of Eq. (8), we also explicitly show that the initialization fidelity  $(1 + e^{-\beta\Delta E})^{-N}$  remains an upper bound to the attainable fidelity  $\mathcal{F}(\rho_1, \sigma_1)$  of the final computation in case the nonunitary map  $\Phi$  is a depolarizing quantum channel. Depolarizing channels are commonly used to model noisy quantum circuits [44,45]. Specifically, it can be proved (see the SM [43] or the proof) that  $\mathcal{F}(\rho_1, \sigma_1) \leq (1 + e^{-\beta\Delta E})^{-N}$ , where  $\rho_1 = \Phi(U\rho_0U^\dagger)$  and  $\sigma_1 = U\sigma_0U^\dagger$  as above.

To better understand our results, we provide a quantitative gauge of the attainable precision (in terms of the fidelity function) of quantum computing, given a nonzero temperature of the initial qubit states. In this regard, in Fig. 1 one can observe a plot of the fidelity  $\mathcal{F}(\rho_0, \sigma_0)$  with respect to the size  $N$  of a qubit register for some values of the single-qubit error rate  $\eta$ . The latter is related to the effective temperature  $\beta$  by means of the relation  $\eta \equiv 1 - (1 + e^{-\beta\Delta E})^{-1}$ . In Fig. 1 one can observe a quite sharp decay of the fidelity  $\mathcal{F}(\rho_0, \sigma_0)$  as the number  $N$  of qubits increases. This holds even in case the value of the single-qubit error rate  $\eta$  is very small.

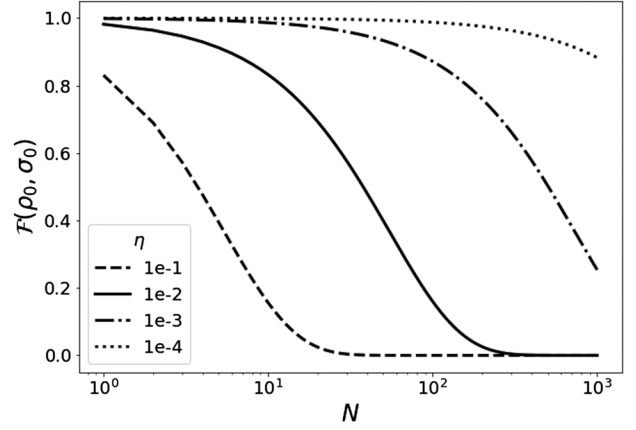


FIG. 1. Scaling of the fidelity  $\mathcal{F}(\rho_0, \sigma_0)$  as a function of the number  $N$  of qubits (in log scale), as predicted by Eq. (4), for different single-qubit error rates  $\eta = 1 - (1 + e^{-\beta\Delta E})^{-1}$ .

Once one realizes that perfect initialization might be challenging due to strict thermodynamic constraints, one must perform quantum state initialization with an error *good enough* to ensure that the fidelity  $\mathcal{F}(\rho_0, \sigma_0)$ —as provided by Eq. (4)—is equal to the target value required for the operation. To put this into perspective, in order to have a target fidelity of 90% for a quantum computer of 1000 qubits, the error on the single-qubit initialization has to be well below  $10^{-4}$ , which, to our knowledge, is the best recorded value [32,33].

*Real data.*—In this section, we aim to understand in quantitative terms how the fidelity of current quantum devices scales as a function of the system’s size and in relation to the quantum state initialization. For this purpose, test runs are performed using a superconducting quantum computer provided by IBM [9]. Specifically, our tests are run on the *ibm-lagos* quantum computer that, with 7 qubits and a quantum volume [46] of 32, was the larger device at our disposal.

The first realized scaling protocol consists in locally measuring the initial register state  $|00\dots 0\rangle$  immediately after its preparation. For each value of  $N$ , the protocol is repeated 5000 times to collect statistics. In this implementation, the fidelity  $\mathcal{F}(\rho_0, \sigma_0)$  is equal to the frequency by which  $|00\dots 0\rangle$  is measured. By performing the protocol for different number  $N$  of qubits, we obtain the results reported in Fig. 2. From the figure one can observe that, while the single-qubit initialization fidelity is almost 99%, as the number of qubits increases this value drops significantly to around 92%. For a quantitative evaluation, we assume the fidelity to be scaling as in Eq. (4), and we fit the value of  $\beta\Delta E$  over the measured data, getting a value of  $\beta\Delta E = 4.35 \pm 0.03$  with a coefficient of determination  $R^2 = 0.976$ . The resulting curve, whose analytical expression is provided by Eq. (4), is plotted as the dashed line in Fig. 2. Since IBM provides us with the values of  $\Delta E$  [9] for each qubit of the employed processor (all around 5 GHz), we can

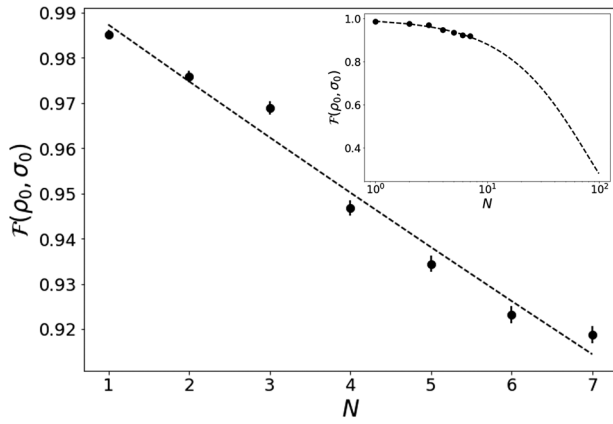


FIG. 2. Measured fidelity values of the state  $\sigma_0$  on the ibm-lagos quantum computer as a function of the number  $N$  of reset qubits. The dashed line denotes the theoretical fit on the measured data using Eq. (4). In the inset, we show the same plot but with the theoretical fit extended to 100 qubits; the log scale on the  $x$  axis is used for visualization purposes. Error bars over the measured values are computed by assuming that error fluctuations follow a Gaussian distribution.

thus compute the effective temperature  $\beta$ , which for the realized test is placed at  $56.80 \pm 1.21$  mK. This effective temperature, as expected, is a bit higher than the physical temperature of the fridge ( $\sim 15$  mK) since it takes into account also the effect of sources of noise such as measurement-induced or single-gate errors. Note that our choice to take a global constant for the effective temperature gives a small discrepancy between the measured values and the theoretical scaling curve, albeit in the real device every qubit should have its own temperature. The trend of the fidelity scaling provided by Eq. (4), versus the size  $N$ , is shown in the inset of Fig. 2, where the predicted fidelity is evaluated for a circuit composed of a larger number of qubits. We remark here that, since the number of qubits at our disposal was just up to  $N = 7$ , this scaling is an extrapolation from our theory and the fit we provide still does not constitute a definitive proof that the scaling we propose is indeed the correct one (it serves as a visual guide of what our bounds predict). However, the fidelity scaling predicted by our theory can be also applied on already published and available data, e.g., for the preparation of GHZ states on trapped ion platforms [47,48] and the sampling from random circuits with fixed depth [1] on a superconducting chip. As discussed in detail in the SM [43] we can use our model to both extrapolate useful information and fit the fidelity values in [1,48] as a function of the number of qubits  $N \in [12, 53]$ . This provides a further validation of our model beyond the 7-qubits regime. Hence, from the results in Fig. 2, it becomes evident the fundamental role played by quantum state initialization and by the effective temperature  $\beta$  of the initial (prepared) state, in order to realize a large-scale quantum computer that maintains acceptable fidelity values.

*Reset protocols.*—We now focus on understanding how these fidelity values can be improved. For such a purpose, active reset methods have been devised that fall into two categories: conditional [49–51] and unconditional [29,52–54] resets. We here employ a mixture of conditional resets methods and thermalization inspired by other works performed by IBM [55] where we take a register of qubits, initially prepared in the superposition state  $|+\rangle^{\otimes N} \equiv H^{\otimes N}|00\dots 0\rangle$  (with  $H$  being the Hadamard gate) [56] and reset to  $|00\dots 0\rangle$  by means of  $K$  consecutive conditional resets. In this conditional reset protocol, each qubit of the register is measured and then a NOT-gate is applied conditionally on the measurement outcome. Ideally, the register would be reset to  $|00\dots 0\rangle$  with zero error, but practically its state is set to the density operator  $\rho_K$ .

In Fig. 3, the results of the conditional reset runs, carried out on the 7-qubits IBM quantum computer ibm-lagos, are plotted for a varying number of resets  $K$ . As one can note, by increasing the number of resets (i.e., by employing more energy to carry out the reset protocol), the state reset fidelity increases up to a certain plateau, whose value depends on (i) the measurement readout error, (ii) the gate noise affecting the NOT operation, and (iii) the thermalization of the qubit due to the external environment. We also observe that we can further increase the fidelity of our reset protocol by inserting a delay of  $500 \mu\text{s}$  between two consecutive resets (dash-dotted lines in Fig. 3) during which the qubits thermalize with the environment. This delay value of  $500 \mu\text{s}$  is the maximum that we could implement on our machine and we observed that in general, for different values, increasing the delay leads to a better reset fidelity. A similar behavior was also observed in [57] for a range of different processors. Moreover, one can see

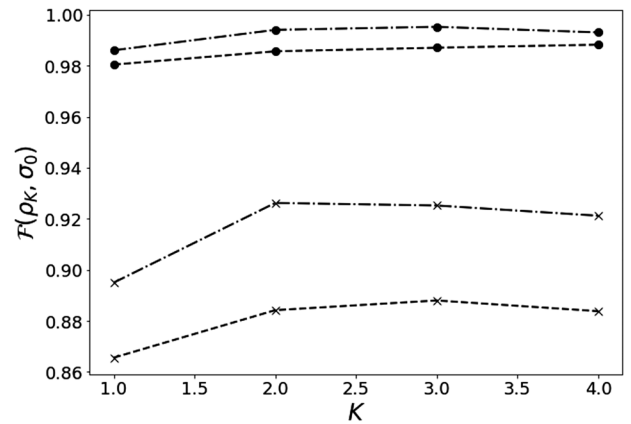


FIG. 3. Measured fidelity between the quantum computational state  $\sigma_0$  and the density operator  $\rho_K$ , solution of the conditional reset protocol, as a function of  $K$ . The circle markers represent conditional resets on a single-qubit register, while the cross markers represent the conditional resets on a 7-qubits register. Dashed lines refer to consecutive resets without delay and dash-dotted lines to resets with a delay of  $500 \mu\text{s}$  between them. The error bars are smaller than the size of the markers.

that the difference between the results provided by the reset protocol applied both to a single-qubit register and to the 7-qubits one lies in the plateau's value (which decreases as the size of the register increases) and not in the number  $K$  of resets needed to reach the maximum allowed fidelity. Our findings hint that achieving greater fidelity values amounts to expending a larger amount of thermodynamic resources in the state initialization protocol, as we quantified in Fig. 3.

*Conclusions.*—To conclude, we investigated how the fidelity of initializing a quantum register, as well as preparing a generic pure quantum state, is constrained by the third law of thermodynamics. The expected scaling follows the one expressed by Eq. (4) for every finite value of the effective inverse temperature  $\beta$  of the initial qubits register. We also observe a scaling compatible to the one in Eq. (4) on a real quantum computer, albeit limited to 7 qubits. The solution to the challenge posed by this constraint is to use better protocols and use more resources in order to reach the target fidelity values needed given the desired size of the quantum register.

In this regard, it would be of great interest to investigate implementations of conditional and unconditional resets, as well as ideas that avoid resets entirely [58]. A detailed study of all the variants of qubit reset would be timely and of great importance to the future of quantum computing. In future investigations, one could also explore whether quantum computing can be redesigned to operate (even partially) on mixed quantum states [59]. In conclusion, we would like to stress the relevance that the thermodynamic study of quantum systems will have for the development of quantum devices and the successful realization of large-scale quantum computers [12,60–62]. As we showed in this Letter, considerations about energy dissipation, finite-temperature states, and other thermodynamic quantities will be key aspects for the next developments in practical applications of quantum computing.

We gratefully thank Per Delsing, Thomas Monz, and Michele Campisi for pointing out useful references and fruitful discussions. We also acknowledge the access to advanced services provided by the IBM Quantum Researchers Program. The views expressed are those of the authors and do not reflect the official policy or position of IBM or the IBM Quantum team. E. Z. C. and Y. O. acknowledge the support from FCT—Fundação para a Ciência e a Tecnologia (Portugal), namely through project UIDB/50008/2020 and UIDB/04540/2020, as well as from projects TheBlinQC and QuantHEP supported by the EU H2020 QuantERA ERA-NET Cofund in Quantum Technologies and by FCT (QuantERA/0001/2017 and QuantERA/0001/2019, respectively), and from the EU H2020 Quantum Flagship project QMiCS (820505). S. G. acknowledges the Blanceflor Foundation for financial support through the project “The thermodynamics behind the measurement postulate of quantum mechanics (TRIESTE).”

- [1] F. Arute, K. Arya, R. Babbush *et al.*, Quantum supremacy using a programmable superconducting processor, *Nature (London)* **574**, 505 (2019).
- [2] Y. Wu, W. Bao, S. Cao *et al.*, Strong Quantum Computational Advantage Using a Superconducting Quantum Processor, *Phys. Rev. Lett.* **127**, 180501 (2021).
- [3] R. Kueng, D. M. Long, A. C. Doherty, and S. T. Flammia, Comparing Experiments to the Fault-Tolerance Threshold, *Phys. Rev. Lett.* **117**, 170502 (2016).
- [4] E. Nielsen, J. K. Gamble, K. Rudinger, T. Scholten, K. Young, and R. Blume-Kohout, Gate set tomography, *Quantum* **5**, 557 (2021).
- [5] R. Raussendorf, Key ideas in quantum error correction, *Phil. Trans. R. Soc. A* **370**, 4541 (2012).
- [6] S. J. Devitt, W. J. Munro, and K. Nemoto, Quantum error correction for beginners, *Rep. Prog. Phys.* **76**, 076001 (2013).
- [7] E. Knill, R. Laflamme, and W. H. Zurek, Resilient quantum computation, *Science* **279**, 342 (1998).
- [8] D. Aharonov and M. Ben-Or, Fault-tolerant quantum computation with constant error rate, *SIAM J. Comput.* **38**, 1207 (2008).
- [9] <https://quantum-computing.ibm.com/>, Visited on 2022.
- [10] E. A. Sete, W. J. Zeng, and C. T. Rigetti, A functional architecture for scalable quantum computing, in *2016 IEEE International Conference on Rebooting Computing (ICRC)* (IEEE, 2016), pp. 1–6.
- [11] K. Wright, K. M. Beck, S. Debnath *et al.*, Benchmarking an 11-qubit quantum computer, *Nat. Commun.* **10**, 5464 (2019).
- [12] V. Cimini, S. Gherardini, M. Barbieri, I. Gianani, M. Sbroscia, L. Buffoni, M. Paternostro, and F. Caruso, Experimental characterization of the energetics of quantum logic gates, *npj Quantum Inf.* **6**, 96 (2020).
- [13] J. Stevens, D. Szombati, M. Maffei *et al.*, Energetics of a Single Qubit Gate, *Phys. Rev. Lett.* **129**, 110601 (2022).
- [14] L. Buffoni and M. Campisi, Thermodynamics of a quantum annealer, *Quantum Sci. Technol.* **5**, 035013 (2020).
- [15] M. Campisi and L. Buffoni, Improved bound on entropy production in a quantum annealer, *Phys. Rev. E* **104**, L022102 (2021).
- [16] M. Fellous-Asiani, J. H. Chai, R. S. Whitney, A. Auffèves, and H. K. Ng, Limitations in quantum computing from resource constraints, *PRX Quantum* **2**, 040335 (2021).
- [17] W. Nernst, Über die Beziehungen zwischen Wärmeentwicklung und maximaler Arbeit bei kondensierten Systemen, *Ber. Kgl. Pr. Akad. Wiss.* **52**, 933 (1906).
- [18] Y. Guryanova, N. Friis, and M. Huber, Ideal projective measurements have infinite resource costs, *Quantum* **4**, 222 (2020).
- [19] F. Ticozzi and L. Viola, Quantum resources for purification and cooling: Fundamental limits and opportunities, *Sci. Rep.* **4**, 1 (2014).
- [20] P. Taranto, F. Bakhshinezhad, A. Bluhm *et al.*, Landauer vs. Nernst: What is the true cost of cooling a quantum system?, [arXiv:2106.05151](https://arxiv.org/abs/2106.05151).
- [21] J. J. Pla, K. Y. Tan, J. P. Dehollain, W. H. Lim, J. J. L. Morton, D. N. Jamieson, A. S. Dzurak, and A. Morello, A single-atom electron spin qubit in silicon, *Nature (London)* **489**, 541 (2012).

- [22] J. J. Longdell and M. J. Sellars, Experimental demonstration of quantum-state tomography and qubit-qubit interactions for rare-earth-metal-ion-based solid-state qubits, *Phys. Rev. A* **69**, 032307 (2004).
- [23] B. Lauritzen, S. R. Hastings-Simon, H. De Riedmatten, Mikael Afzelius, and Nicolas Gisin, State preparation by optical pumping in erbium-doped solids using stimulated emission and spin mixing, *Phys. Rev. A* **78**, 043402 (2008).
- [24] T. Utikal, E. Eichhammer, L. Petersen, A. Renn, S. Götzinger, and V. Sandoghdar, Spectroscopic detection and state preparation of a single praseodymium ion in a crystal, *Nat. Commun.* **5**, 3627 (2014).
- [25] S. Baier, C. E. Bradley, T. Middelburg, V. V. Dobrovitski, T. H. Taminiau, and R. Hanson, Orbital and Spin Dynamics of Single Neutrally-Charged Nitrogen-Vacancy Centers in Diamond, *Phys. Rev. Lett.* **125**, 193601 (2020).
- [26] J. E. Johnson, Christopher Macklin, D. H. Slichter, R. Vijay, E. B. Weingarten, John Clarke, and Irfan Siddiqi, Heralded State Preparation in a Superconducting Qubit, *Phys. Rev. Lett.* **109**, 050506 (2012).
- [27] D. Ristè, C. C. Bultink, Konrad W. Lehnert, and L. DiCarlo, Feedback Control of a Solid-State Qubit Using High-Fidelity Projective Measurement, *Phys. Rev. Lett.* **109**, 240502 (2012).
- [28] M. Partanen, K. Y. Tan, S. Masuda, J. Govenius, R. E. Lake, M. Jenei, L. Grönberg, J. Hassel, S. Simbierowicz, V. Vesterinen *et al.*, Flux-tunable heat sink for quantum electric circuits, *Sci. Rep.* **8**, 1 (2018).
- [29] P. Magnard, P. Kurpiers, B. Royer, T. Walter, J.-C. Besse, S. Gasparinetti, M. Pechal, J. Heinsoo, S. Storz, A. Blais *et al.*, Fast and Unconditional All-Microwave Reset of a Superconducting Qubit, *Phys. Rev. Lett.* **121**, 060502 (2018).
- [30] M. Pierre, I.-M. Svensson, S. R. Sathyamoorthy, G. Johansson, and P. Delsing, Storage and on-demand release of microwaves using superconducting resonators with tunable coupling, *Appl. Phys. Lett.* **104**, 232604 (2014).
- [31] K. Y. Tan, M. Partanen, R. E. Lake, J. Govenius, S. Masuda, and M. Möttönen, Quantum-circuit refrigerator, *Nat. Commun.* **8**, 1 (2017).
- [32] A. H. Myerson, D. J. Szwer, S. C. Webster, D. T. C. Allcock, M. J. Curtis, G. Imreh, J. A. Sherman, D. N. Stacey, A. M. Steane, and D. M. Lucas, High-Fidelity Readout of Trapped-Ion Qubits, *Phys. Rev. Lett.* **100**, 200502 (2008).
- [33] A. H. Burrell, D. J. Szwer, S. C. Webster, and D. M. Lucas, Scalable simultaneous multiqubit readout with 99.99% single-shot fidelity, *Phys. Rev. A* **81**, 040302(R) (2010).
- [34] P. Schindler, J. T. Barreiro, T. Monz, V. Nebendahl, D. Nigg, M. Chwalla, M. Hennrich, and R. Blatt, Experimental repetitive quantum error correction, *Science* **332**, 1059 (2011).
- [35] T. P. Harty, D. T. C. Allcock, C. J. Ballance, L. Guidoni, H. A. Janacek, N. M. Linke, D. N. Stacey, and D. M. Lucas, High-Fidelity Preparation, Gates, Memory, and Readout of a Trapped-Ion Quantum Bit, *Phys. Rev. Lett.* **113**, 220501 (2014).
- [36] R. Jozsa, Fidelity for mixed quantum states, *J. Mod. Opt.* **41**, 2315 (1994).
- [37] J. A. Miszczak, Z. Puchała, P. Horodecki *et al.*, Sub- and super-fidelity as bounds for quantum fidelity, *Quantum Inf. Comput.* **9** (2019).
- [38] M. A. Nielsen, A simple formula for the average gate fidelity of a quantum dynamical operation, *Phys. Lett. A* **303**, 249 (2002).
- [39] T. Geisel, R. Ketzmerick, and G. Petschel, *Quantum Chaos: Between Order and Disorder* (Cambridge University Press, Cambridge, England, 1995), Chap. 1, p. 17.
- [40] A. Beekman, L. Rademaker, and J. van Wezel, An introduction to spontaneous symmetry breaking, *SciPost Phys. Lect. Notes* **11** (2019). [10.21468/SciPostPhysLectNotes.11](https://doi.org/10.21468/SciPostPhysLectNotes.11)
- [41] S. Gherardini, G. Giachetti, S. Ruffo, and A. Trombettoni, Thermalization processes induced by quantum monitoring in multilevel systems, *Phys. Rev. E* **104**, 034114 (2021).
- [42] L. Buffoni and M. Campisi, Spontaneous fluctuation-symmetry breaking and the landauer principle, *J. Stat. Phys.* **186**, 31 (2022).
- [43] See Supplemental Material at <http://link.aps.org/supplemental/10.1103/PhysRevLett.129.150602> for the detailed proofs of the results, and additional analysis on available data.
- [44] E. Knill, Quantum computing with realistically noisy devices, *Nature (London)* **434**, 39 (2005).
- [45] K. s Georgopoulos, C. Emary, and P. Zuliani, Modeling and simulating the noisy behavior of near-term quantum computers, *Phys. Rev. A* **104**, 062432 (2021).
- [46] A. W. Cross, L. S. Bishop, S. Sheldon, P. D. Nation, and J. M. Gambetta, Validating quantum computers using randomized model circuits, *Phys. Rev. A* **100**, 032328 (2019).
- [47] T. Monz, P. Schindler, J. T. Barreiro, M. Chwalla, D. Nigg, W. A. Coish, M. Harlander, W. Hänsel, M. Hennrich, and R. Blatt, 14-Qubit Entanglement: Creation and Coherence, *Phys. Rev. Lett.* **106**, 130506 (2011).
- [48] I. Pogorelov, T. Feldker, Ch. D. Marciniak, L. Postler, G. Jacob, O. Kriegelsteiner, V. Podlesnic, M. Meth, V. Negnevitsky, M. Stadler, B. Höfer, C. Wächter, K. Lakhmanskiy, R. Blatt, P. Schindler, and T. Monz, Compact ion-trap quantum computing demonstrator, *PRX Quantum* **2**, 020343 (2021).
- [49] T. Walter, P. Kurpiers, S. Gasparinetti, P. Magnard, A. Potočnik, Y. Salathé, M. Pechal, M. Mondal, M. Oppliger, C. Eichler *et al.*, Rapid High-Fidelity Single-Shot Dispersive Readout of Superconducting Qubits, *Phys. Rev. Applied* **7**, 054020 (2017).
- [50] D. Ristè, J. G. van Leeuwen, H.-S. Ku, K. W. Lehnert, and L. DiCarlo, Initialization by Measurement of a Superconducting Quantum Bit Circuit, *Phys. Rev. Lett.* **109**, 050507 (2012).
- [51] L. C. G. Govia and F. K. Wilhelm, Unitary-Feedback-Improved Qubit Initialization in the Dispersive Regime, *Phys. Rev. Applied* **4**, 054001 (2015).
- [52] K. Geerlings, Z. Leghtas, I. M. Pop, S. Shankar, L. Frunzio, R. J. Schoelkopf, M. Mirrahimi, and M. H. Devoret, Demonstrating a Driven Reset Protocol for a Superconducting Qubit, *Phys. Rev. Lett.* **110**, 120501 (2013).
- [53] D. J. Egger, M. Werninghaus, M. Ganzhorn, G. Salis, A. Fuhrer, P. Mueller, and S. Filipp, Pulsed Reset Protocol for Fixed-Frequency Superconducting Qubits, *Phys. Rev. Applied* **10**, 044030 (2018).

- 
- [54] A.Z. Goldberg and K. Heshami, Breaking the limits of purification: Postselection enhances heat-bath algorithmic cooling, [arXiv:2108.08853v2](https://arxiv.org/abs/2108.08853v2).
- [55] [https://quantum-computing.ibm.com/lab/docs/iql/manage/systems/reset/backend\\_reset](https://quantum-computing.ibm.com/lab/docs/iql/manage/systems/reset/backend_reset), Visited on 2022.
- [56] We could also use the results of any previous quantum computation, leaving the processor in a state  $|\psi\rangle$  and setting the variable `init_qubits = false`.
- [57] [https://nonhermitian.org/posts/2021/2021-11-07-rep\\_delay.html](https://nonhermitian.org/posts/2021/2021-11-07-rep_delay.html), Visited on 2022.
- [58] M. Werninghaus, D.J. Egger, and S. Filipp, High-speed calibration and characterization of superconducting quantum processors without qubit reset, *PRX Quantum* **2**, 020324 (2021).
- [59] M. Siomau and S. Fritzsche, Quantum computing with mixed states, *Eur. Phys. J. D* **62**, 449 (2011).
- [60] M. Aifer and S. Deffner, From quantum speed limits to energy-efficient quantum gates, *New J. Phys.* **24**, 055002 (2022).
- [61] A. Auffèves, Quantum technologies need a quantum energy initiative, *PRX Quantum* **3**, 020101 (2022).
- [62] C. Cafaro, S. Ray, and P.M. Alsing, Complexity and efficiency of minimum entropy production probability paths from quantum dynamical evolutions, *Phys. Rev. E* **105**, 034143 (2022).